

# Simultaneous production of lepton pairs in ultraperipheral relativistic heavy ion collisions

E. Kurban\* and M. C. Güçlü†

*Department of Physics, Istanbul Technical University, Maslak-Istanbul, Turkey*

(Received 24 August 2017; published 25 October 2017)

We calculate the total cross sections and probabilities of electromagnetic productions of electron, muon, and tauon pairs simultaneously. At the CERN Large Hadron Collider (LHC), the available electromagnetic energy is sufficient to produce all kinds of leptons coherently. The masses of muons and tauons are large, so their Compton wavelengths are small enough to interact with the colliding nuclei. Therefore, the realistic nuclear form factors are included in the calculations of electromagnetic pair productions. The cross section calculations show that, at LHC energies, the probabilities of simultaneous productions of all kinds of leptons are increased significantly compared to energies available at the BNL Relativistic Heavy Ion Collider (RHIC). Experimentally, observing this simultaneous production can give us important information about strong QED.

DOI: [10.1103/PhysRevC.96.044913](https://doi.org/10.1103/PhysRevC.96.044913)

## I. INTRODUCTION

Peripheral collisions of heavy ions have been studied for a long time [1–8] since these types of collisions contain interesting physics problems such as lepton pair, coherent or incoherent vector-meson, and some other exotic particle productions. Very strong electromagnetic fields are produced near peripheral heavy ion collisions at relativistic velocities. The electromagnetic fields are proportional to Lorentz factor  $\gamma$ , beam kinetic energy per nucleon, and the charge of the ion  $Z$ . This electromagnetic field contains many virtual photons, which are the source of lepton pair production and different types of photonuclear interactions.

An exact solution of the time-dependent Dirac equation for ionization and pair production induced by ultrarelativistic heavy ion collisions was done in Ref. [9]. This exact method could be used for other applications related to electromagnetic lepton pairs in the future. The perturbative cross section for free electron-positron pair production at the BNL Relativistic Heavy Ion Collider (RHIC) is about 30 000 b. On the other hand, since the large number of energy and angular momentum states are coupled, nonperturbative approaches for this process have difficulties; however, the method in Ref. [9] seems to make the problem solvable.

The RHIC and the CERN Large Hadron Collider (LHC) are designed to collide fully ionized heavy ions in the center-of-mass frame with 100 and 3400 GeV energies per nucleon, respectively. Many calculations have been done for RHIC energies for the electromagnetic production of lepton pairs. Nowadays we have also the LHC, and its available energy is much larger than that at the RHIC. The parameters which are related to the RHIC and the LHC are listed in Tables I and II. The critical electric field to produce a lepton pair and the maximum electric field for one of the heavy ions can be given as

$$E_{\text{crit}} \approx \frac{(mc^2)^2}{e\hbar c}, \quad E_{\text{max}} \approx \frac{Ze\gamma}{b^2}. \quad (1)$$

Therefore, cross sections of lepton pair production, especially heavy lepton pair production, become quite large and cannot be ignored.

In the past, several calculations have been done for the single pair production of leptons:

$$Z + Z \rightarrow Z + Z + l^+l^-, \quad l = e, \mu, \tau. \quad (2)$$

Since the mass of an electron (0.511 MeV) is much smaller than a muon (105.66 MeV) and a tauon (1784 MeV), and the Compton wavelength of an electron (386 fm) is much larger than a muon (1.86 fm) and a tauon (0.11 fm), the cross sections of producing electron pairs are much larger than for heavy leptons. In addition to this, since the Compton wavelengths of muons and tauons are smaller than the radius of the colliding heavy ions (Au, Pb), nucleon [4,10] and nucleus form factors are not negligible. Therefore, the realistic charge form factors play important roles in calculating the cross sections of the heavy lepton pair productions.

In this work, we have calculated the cross section of simultaneous production of all three lepton pairs together:

$$Z + Z \rightarrow Z + Z + e^+e^- + \mu^+\mu^- + \tau^+\tau^-. \quad (3)$$

The main motivation for this calculation is that the available energy in this collision is sufficient to create all these lepton pairs simultaneously. Especially at LHC energies, interesting processes can occur, and these processes can help us to understand strong QED. One approach is to observe different physical processes simultaneously. For example, the STAR Collaboration measured the electron-positron pairs [11] together with the electromagnetic excitation of both ions, predominantly due to the giant dipole resonance. The STAR Collaboration used gold atoms at  $\sqrt{s} = 200$  GeV/nucleon energies. The decay of the excited nucleus generally emits one or two neutrons, and these neutrons are detected in the forward zero-degree calorimeter.

For sufficiently high energies, the production of the cross section for a single pair becomes large. At LHC energies, the probabilities for producing multiple pairs of leptons become important contributions to the measured cross sections. In addition to this, the perturbative result for single-pair production violates unitarity of the cross section for large  $Z$

\*erknurban@gmail.com

†guclu@itu.edu.tr

TABLE I. The critical energies and electric fields that can produce leptons.  $\lambda_c$  is the Compton wavelength of the corresponding lepton.

Lepton	$\hbar\omega_{\text{crit}} = 2mc^2$ (MeV)	$\lambda_c$ (fm)	$E_{\text{crit}}$ (V/m)
$e^\pm$	1.02	386.2	$1.3 \times 10^{18}$
$\mu^\pm$	211.4	1.87	$5.7 \times 10^{22}$
$\tau^\pm$	3568	0.11	$1.6 \times 10^{25}$

and high energies. Multiple-pair production processes solve this single-pair production problem. Through the Poisson expression, the multiple-pair production cross sections can be obtained. Experimentally [12], only upper limits have been achieved for the measurements of multiple-pair productions so far.

In ultrarelativistic heavy ion collisions, there are two dominant processes that restrict the luminosity of the ion beams. One of them is bound-free electron-positron pair production (BFPP) that occurs with the capture of the electron after the free electron-positron pair production, while the positron goes its way freely. In the bound-free pair production process, the produced particle especially is captured in the  $1s$  ground state of one of the ions. The captured electron by one of the colliding ions leads to a change in the charge and mass of the ions and causes the ion to fall out of the beam. In this case, the ion that captures the particle exits from the beam. This process leads to beam depletion. The calculation of the electron capture process is important for the lifetime of the beam. Recent calculations show that electron capture and giant dipole resonance play important roles in the beam luminosity [13,14].

In collisions of relativistic heavy ions, leptons are produced not only through the electromagnetic process but also by hadronic interactions. These leptons, which are produced by the Drell-Yan process, are a possible signal of the quark-gluon plasma. However, the electromagnetically produced lepton-pair cross section, especially for electron-positron pairs, is very large, and therefore can mask the leptons originating from the quark-gluon plasma. Therefore, it is very important to know the electromagnetic lepton pair production cross section in order to separate these two processes and minimize confusion.

## II. FORMALISM

Figure 1 shows the collisions of ions where  $\beta$  and  $-\beta$  represent the velocities of two heavy ions, nucleus 1 and

TABLE II. The first line in the table shows the maximum electric field of the colliding heavy ions at RHIC and LHC. Other lines are the ratio of between maximum electric field and the critical electric field of producing corresponding lepton.

Parameter	RHIC	LHC
$E_{\text{max}}$ (V/m)	$\sim 2 \times 10^{23}$	$\sim 7 \times 10^{24}$
$E_{\text{max}}/E_{\text{crit}}(e^\pm)$	$1.5 \times 10^5$	$5.3 \times 10^6$
$E_{\text{max}}/E_{\text{crit}}(\mu^\pm)$	3.5	123.7
$E_{\text{max}}/E_{\text{crit}}(\tau^\pm)$	0.01	0.4

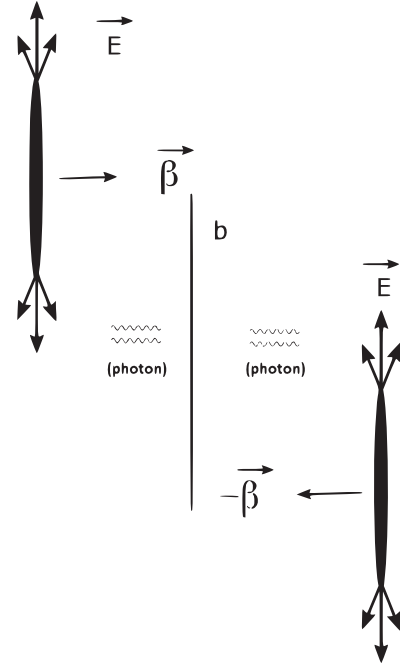


FIG. 1. Relativistic collision of two heavy ion is illustrated as schematic diagram. Impact parameter between the ions is  $b$ , and the Lorentz contracted electric field is also shown.

nucleus 2, respectively. The velocities are parallel to the  $z$  axis and the distance line shows the impact parameter between the center of nucleus 1 and the center of nucleus 2. In Fig. 2, second order Feynman diagrams are shown for various simultaneous production of lepton pairs from the electromagnetic fields of heavy ions.

The semiclassical coupling of leptons to the electromagnetic field is represented by the Lagrangian density, which only depends on the classical four-vector potential  $A^\mu$  and also conserves lepton number:

$$L_{\text{int}}(x) = -\bar{\psi}\gamma_\mu\psi(x)A^\mu(x), \quad (4)$$

where we can write the  $A^\mu$  as the sum of two heavy ions,

$$A^\mu(q; b) = A^\mu(1; q; b) + A^\mu(2; q; b). \quad (5)$$

We can also write the components of the potential from both nuclei in momentum space as

$$A_0^{(1,2)}(q; b) = -8\pi^2 Z\delta(q_0 \mp \beta q_z) f_z(q^2) \frac{\exp(\pm i q_\perp b/2)}{q_z^2 + \gamma^2 q_\perp^2}, \quad (6)$$

$$A_x^{(1,2)}(q) = 0, \quad (7)$$

$$A_y^{(1,2)}(q) = 0, \quad (8)$$

$$A_z^{(1,2)}(q) = \pm\beta A_0^{(1,2)}(q) \quad (9)$$

where  $f_z(q^2)$  is the form factor of the nucleus. These form factors play an important role in heavy lepton pair productions. We have used the two-parameter Fermi (2pF) function (or Woods-Saxon function) for the charge distribution of the

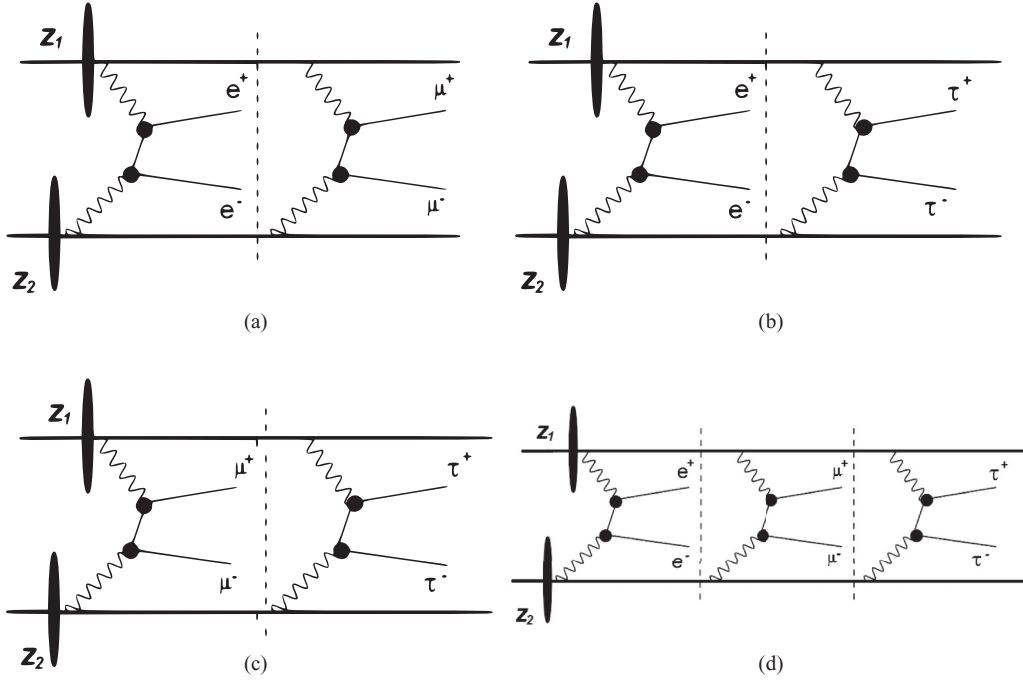


FIG. 2. Second-order Feynman diagrams for simultaneous (a) electron and muon pair production, (b) electron and tauon pair production, (c) muon and tauon pair production, and (d) electron, muon, and tauon pair production.

protons:

$$\rho(r) = \frac{\rho_0}{1 + \exp[(r - R)/R_0]}, \quad (10)$$

where  $R$  is the radius of the nucleus and  $R_0$  is the skin depth or diffuseness parameter. These parameters are obtained by fits to the electron scattering data [15] and  $\rho_0$  is written by the normalization condition. For symmetric nuclei, the nuclear density for a nucleus that has mass number  $A$  and distance  $r$  from its center is modeled in the literature with a Woods-Saxon distribution as in Eq. (10), where  $\rho_0 = \frac{0.1694}{A} \text{ fm}^{-3}$  for the Au nucleus and  $\rho_0 = \frac{0.1604}{A} \text{ fm}^{-3}$  for the Pb nucleus. The radii of the gold and lead nuclei are equal to  $R_{Au} = 6.38 \text{ fm}$  and  $R_{Pb} = 6.62 \text{ fm}$  respectively. In order to see the effects of the proton distributions in the nucleus, we need to have an analytical expression of the Fourier transforms of the Woods-Saxon distribution:

$$f_Z(q^2) = \int_0^\infty \frac{4\pi}{q} \rho(r) \sin(qr) dr, \quad (11)$$

where  $f_Z(q^2)$  is plotted in Fig. 3. It is clearly seen that the analytic expression and the numerical calculation are nearly identical.

Including all these equations and definitions, we can write the total cross section of free lepton pair production as

$$\sigma = \int d^2b \sum_{k>0} \sum_{q<0} |\langle \chi_k^+ | S | \chi_q^- \rangle|^2, \quad (12)$$

where  $S$  is the scattering matrix,  $|\chi_k^+\rangle$  and  $|\chi_q^-\rangle$  are single-particle and single-antiparticle states respectively. By following the steps used in Refs. [1,3,16], the lepton pair

production cross section can be written as

$$\sigma = \frac{1}{4\beta^2} \sum_{\sigma_k} \sum_{\sigma_q} \int \frac{dk_z dq_z d^2 p_\perp}{(2\pi)^4} \int \frac{d^2 k_{1\perp} d^2 q_{2\perp}}{(2\pi)^4} \times |F(k_\perp - p_\perp; w_1) F(k_\perp - p_\perp; w_2) T(p_\perp : +\beta) + F(k_\perp - p_\perp; w_2) F(k_\perp - p_\perp; w_1) T(p_\perp : -\beta)|^2. \quad (13)$$

The frequencies  $\omega_1$  and  $\omega_2$  are from the heavy ions 1 and 2, respectively. The summation over  $k$  is valid for the positive energy states, and the summation over  $q$  is limited to the

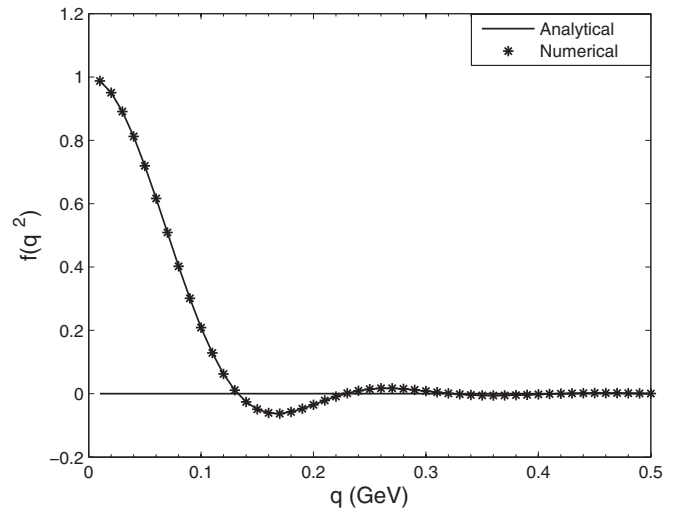


FIG. 3. The electromagnetic form factor for gold. The solid line is the analytic form of the Woods-Saxon distribution and the starred line is the numerical calculation of the same equation.

negative energy states in the Dirac sea.  $k_z$  and  $q_z$  are the longitudinal momenta and  $k_\perp$  and  $q_\perp$  are transverse momenta of the produced leptons and antileptons, respectively. In addition to this,  $p_\perp$  is the transverse momentum of the intermediate states; however, longitudinal momenta of the intermediate states  $p_z$  are fixed by the momentum conservation. Finally, we can write the reduced Feynman amplitude  $T(p_\perp; \beta)$  as

$$T(p_\perp; \beta) = \sum_s \sum_{\sigma_p} \{E_p^{(s)} - [E_k^{(+)} / 2 + \beta(k_z - q_z) / 2]\}^{-1} \\ \times \langle u_{\sigma_k}^{(+)} | (1 - \beta \alpha_z) | u_{\sigma_p}^{(s)} \rangle \langle u_{\sigma_p}^{(s)} | (1 + \beta \alpha_z) | u_{\sigma_q}^{(-)} \rangle, \quad (14)$$

and  $F(q : w)$  is the scalar part of the field from the heavy ions:

$$F(q : w) = \frac{4\pi Z\gamma^2 \beta^2}{w^2 + \beta^2 \gamma^2 |q|^2} f_Z(q^2), \quad (15)$$

$$\mathcal{F}(q) = \frac{\pi}{8\beta^2} \sum_{\sigma_k} \sum_{\sigma_q} \int_0^{2\pi} d\phi_q \int \frac{dk_z dq_z d^2 k_\perp d^2 Q}{(2\pi)^{10}} \left\{ \left[ F\left(\frac{Q-q}{2}; w_1\right) F(-K; w_2) T\left(k_\perp - \frac{Q-q}{2}; \beta\right) \right. \right. \\ \left. \left. + F\left(\frac{Q-q}{2}; w_1\right) F(-K; w_2) T(k_\perp - K; -\beta) \right] \left[ F\left(\frac{Q+q}{2}; w_1\right) F(-q-K; w_2) T\left(k_\perp - \frac{Q+q}{2}; \beta\right) \right. \right. \\ \left. \left. + F\left(\frac{Q+q}{2}; w_1\right) F(-q-K; w_2) T(k_\perp + q - K; -\beta) \right] \right\}, \quad (17)$$

where  $\mathcal{F}(q)$  function is calculated by Monte Carlo technique for a fixed value of  $q$ . When the technique is implemented for Au+Au collisions at 3400 and 100 GeV energies, the behavior of the function is obtained as an exponential form. We have used sufficient Monte Carlo points for adequate accuracy to obtain the  $F(q)$  function. A smooth function

$$\mathcal{F}(q) = \mathcal{F}(0) e^{-aq} = \sigma_T e^{-aq} \quad (18)$$

is then fit to the calculated values to obtain the  $a$  values tabulated in Table III.  $\mathcal{F}(0)$  correspond to the total cross section at  $q = 0.0$  and  $a$  is the slope of the function. After determining the  $\mathcal{F}(q)$  function, we can insert it into Eq. (16),

$$\frac{d\sigma}{db} = \mathcal{F}(0) \int_0^\infty dq qb J_0(qb) e^{-aq} = \sigma_T \frac{ab}{(a^2 + b^2)^{3/2}}, \quad (19)$$

and obtain a smooth and well behaved impact parameter dependence cross section expression. This equation is valid for all kind of leptons. The values of  $a$  and the total cross

TABLE III. Values obtained for electron, muon, and tauon pairs at 100 and 3400 GeV.  $\lambda_c^e$ ,  $\lambda_c^\mu$ , and  $\lambda_c^\tau$  are Compton wavelengths for the electron, muon, and tauon respectively.

Lepton pair	100 GeV	3400 GeV
$e^\pm$	$5.30 \lambda_c^e$	$12.55 \lambda_c^e$
$\mu^\pm$	$13.85 \lambda_c^\mu$	$19.24 \lambda_c^\mu$
$\tau^\pm$	$84 \lambda_c^\tau$	$187.57 \lambda_c^\tau$

where  $f_Z(q^2)$  is the nuclear form factor defined in Eq. (11) and  $u_{\sigma_p}^{(s)}$  is the spinor part of the states  $\chi^{(s)}$ .

Equation (13) gives us the total cross section integrated over the impact parameters. However, if the impact parameter dependence cross section is needed, then we should keep the impact parameter and integrate the cross section equation over all variables. When we do this, we can obtain the equation in the form

$$\frac{d\sigma}{db} = \int_0^\infty dq qb J_0(qb) \mathcal{F}(q), \quad (16)$$

where the equation includes the zeroth-order Bessel function. This Bessel function oscillates rapidly for large  $b$  values, therefore Monte Carlo techniques cannot be applied here. To solve the integral, the integration is divided into parts and calculated separately:

section  $\sigma_T$  are different for electrons, muons, and tauons, and they are tabulated in Tables III and IV.

The lowest order perturbative result of the probability can be written as

$$\mathcal{P}(b) = \sum_{k>0} \sum_{q<0} |\langle X_k^+ | \mathcal{S} | X_q^- \rangle|^2, \quad (20)$$

which is equal to

$$\mathcal{P}(b) = \frac{1}{2\pi b} \frac{d\sigma}{db} = \sigma_T \frac{a}{2\pi(a^2 + b^2)^{3/2}}. \quad (21)$$

TABLE IV. Total cross section values are shown for lepton pairs at RHIC and LHC. The first group of rows shows production of electron, muon, and tauon pairs separately, while the second group of rows shows production of two different types lepton pairs at the same time. The last row shows production of electron-muon-tauon pairs at the same time.

Lepton pairs	Total cross section at RHIC (barn)	Total cross section at LHC (barn)
$e^\pm$	34566	210254
$\mu^\pm$	0.2	2.3
$\tau^\pm$	$3.7 \times 10^{-6}$	$1.4 \times 10^{-3}$
$e^\pm\text{-}\mu^\pm$	0.039	0.22
$e^\pm\text{-}\tau^\pm$	$7.3 \times 10^{-7}$	$9.4 \times 10^{-5}$
$\mu^\pm\text{-}\tau^\pm$	$9.6 \times 10^{-9}$	$1.2 \times 10^{-5}$
$e^\pm\text{-}\mu^\pm\text{-}\tau^\pm$	$1.92 \times 10^{-9}$	$1.1 \times 10^{-6}$

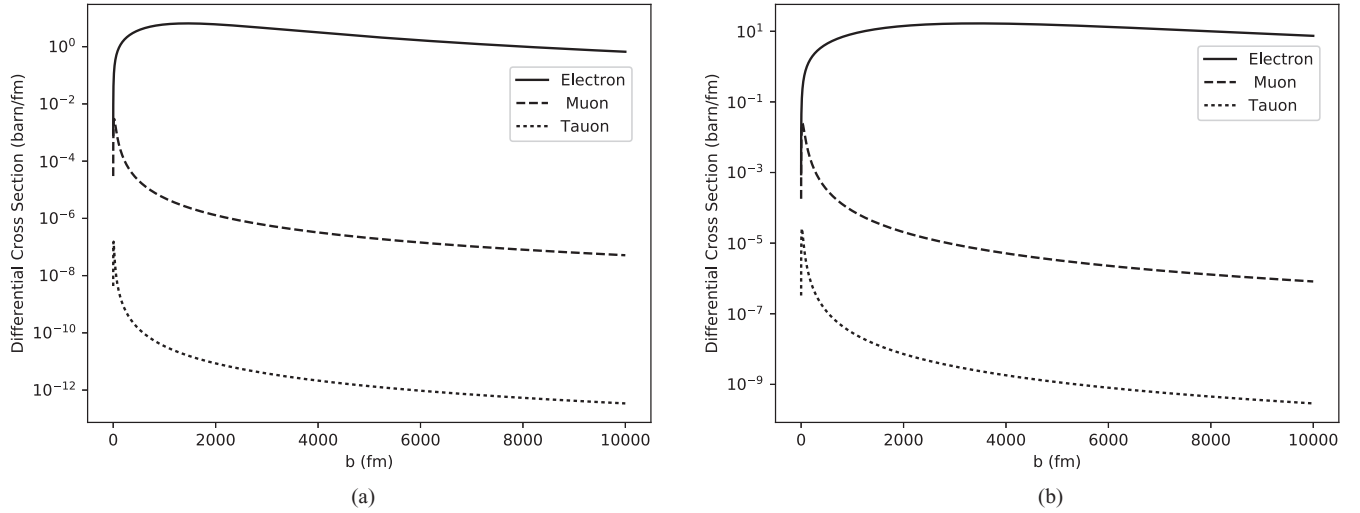


FIG. 4. Impact parameter dependent cross section for lepton pairs produced by Au+Au ion collisions at (a) 100 GeV and (b) 3400 GeV.

However, for small impact parameters and high energies unitarity is violated, so the probability becomes greater than 1. Therefore we can use the Poisson distribution [16–18] whose mean value is  $\mathcal{P}(b)$ ,

$$P_N(b) = \frac{\mathcal{P}(b)^N \exp[-\mathcal{P}(b)]}{N!}, \quad (22)$$

where  $N$  is number of pairs. In order to obtain the one-pair cross section ( $N = 1$ )  $\sigma_{1 \text{ pair}}$ , we simply integrate the one-pair probability over the impact parameter  $b$ :

$$\sigma_{1 \text{ pair}} = \int d^2b P_1(b). \quad (23)$$

Our main task is to calculate the probabilities of more than one type of lepton simultaneously. For this, we can use the factorization method [7,19,20] to calculate  $e\mu, e\tau, \mu\tau$  pair production probabilities as

$$P_1^{l_1 l_2}(b) = \{P_1^e(b)P_1^\mu(b), P_1^e(b)P_1^\tau(b), P_1^\mu(b)P_1^\tau(b)\}, \quad (24)$$

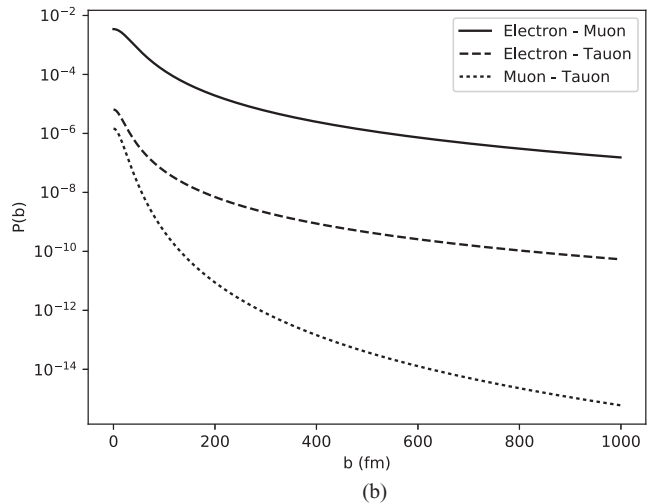
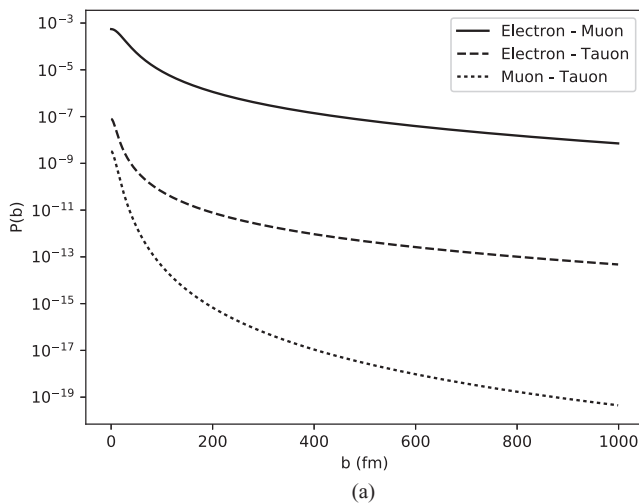


FIG. 5. (a) The behaviors of the probability values are shown depending on impact parameter  $b$  for two of the  $e^\pm\text{-}\mu^\pm\text{-}\tau^\pm$  pairs produced at the same time by Au+Au collisions at (a) 100 GeV and (b) at 3400 GeV.

where  $l_1, l_2 = e, \mu, \tau$ , and these probabilities are plotted in Fig. 5. Similarly, an impact parameter dependent probability of producing three different types of leptons can be written as

$$P_1^{e\mu\tau}(b) = P_1^e(b)P_1^\mu(b)P_1^\tau(b); \quad (25)$$

it is plotted in Fig. 6. For the total cross sections we have to integrate the above probabilities over the impact parameter  $b$ ,

$$\sigma_T^{l_1 l_2} = \int_0^\infty 2\pi b db P_1^{l_1}(b)P_1^{l_2}(b), \quad (26)$$

and for the total cross section of the three types of lepton pair production we have

$$\sigma_T^{e\mu\tau} = \int_0^\infty 2\pi b db P_1^e(b)P_1^\mu(b)P_1^\tau(b). \quad (27)$$

All these calculated total cross sections are tabulated in Table IV.

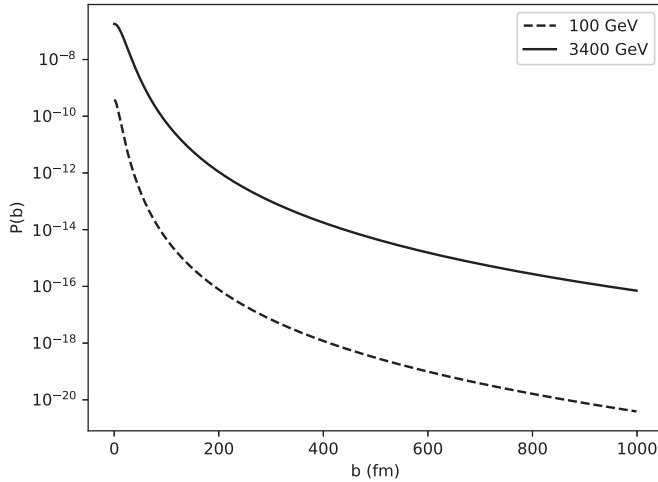


FIG. 6. The probability of lepton pairs being produced at the same time by Au+Au collisions at 100 and 3400 GeV is shown depending on impact parameter  $b$ .

### III. RESULT

In this work, we study the total cross sections, the impact parameter dependent cross sections, and the probabilities of lepton pairs produced by Au+Au collisions at LHC and RHIC energies. We especially focus on the probabilities of different types of lepton pairs that are created simultaneously.

Since the Compton wavelength of the electron is much larger than the radii of the colliding heavy ions, the form factors of the nucleus almost have no effect on the production of electron-positron pairs. On the other hand, the Compton wavelengths of muons and tauons are smaller than the radii of the colliding heavy ions, therefore the effects of the form factors become dominant for pair production. At RHIC and LHC energies, the muon pair production is reduced by factors of about 3 and 2, respectively. On the other hand, at RHIC and LHC energies, the tauon pair production is reduced by factors of about 100 and 5, respectively.

The cross section calculations involve nine-dimensional integrals, and they cannot be calculated analytically, so we have used a Monte Carlo method to calculate the equations numerically. We use  $> 2 \times 10^6$  Monte Carlo points, and we have reached sufficient convergence to obtain the total cross section of electron, muon, and tauon pairs.

In order to calculate the impact parameter dependent cross section, we first obtained values of  $a$  for each type of lepton. The values of  $a$  are tabulated in Table III for all leptons. Once we determined this parameter, all calculations were easily done. In Table IV, we show the total cross sections of production for all combinations of lepton pairs. In the first group of rows we can see the single pair production cross sections. This clearly shows that as lepton mass increases, the cross section decreases rapidly. On the other hand, in the second group of rows, we show the total cross sections of simultaneous production for all combinations of two leptons. These results show that at LHC energies the cross sections are 2 or 4 order of magnitude greater than at RHIC energies. Finally in the last row, the simultaneous total cross sections

TABLE V. The percentages of partial total cross sections of lepton pairs integrated between 2000 fm and  $\infty$ .

Lepton pair	RHIC (%)	LHC (%)
$e^\pm$	72	92
$\mu^\pm$	1	2
$\tau^\pm$	0.5	1

of all three types lepton pairs are written. At LHC energies, the cross section of this production is nearly three order of magnitude greater than at RHIC energies.

The impact parameter dependent cross sections of leptons are drawn in Fig. 4(a) for RHIC and (b) for LHC energies. The behaviors in both figures are nearly the same; however, the impact parameter dependence is enhanced by a one or two orders of magnitude at LHC energies. In Tables I and II, it is clear that the relativistic heavy ions are accompanied by strong electromagnetic fields. In the Weizsäcker-Williams approach, the combined fields of electric and magnetic fields from the ions may be treated as a flux of nearly-real virtual photons. For two ions separated by a large  $b$ , the most favorable pair production point is midway between the two ions. At this point, the maximum photon energy is  $k_{\max} = 2\gamma\hbar c/b$ , where  $\gamma$  is the Lorentz boost of the ion, and  $b$  is the impact parameter, which is the transverse distance from the ion. At the RHIC, for  $b = 2000$  fm,  $k_{\max} = 20$  MeV; and at the LHC  $k_{\max} = 680$  MeV. For the production of  $\tau$  pairs, the impact parameter dependent cross section increased almost by 1000 times from RHIC to LHC energies at the impact parameter 2000 fm; however the ratio of  $k_{\max}$  increased by  $680/20 = 34$ , only. To calculate the percentage of the contribution to the total cross section above 2000 fm, we can use the integration

$$\left( \int_{2000 \text{ fm}}^{\infty} \frac{d\sigma}{db} db \right) / \left( \int_0^{\infty} \frac{d\sigma}{db} db \right), \quad (28)$$

and we can show that the contribution to the total cross section of impact parameters greater than 2000 fm is nearly 0.5% at the RHIC and 1% at the LHC for the  $\tau$  production. This shows that the differential cross sections decrease fast for large impact parameters. Similar calculations are done for all types of leptons, and the results are tabulated in Table V. It is interesting that, for the electron-positron pair production, 72% of the total cross section comes from impact parameters which are greater than 2000 fm at RHIC, and 92% at LHC.

In Fig. 5, we have plotted the impact parameter dependence probabilities of producing two different lepton pairs simultaneously. Again, in these figures the patterns are nearly the same for both RHIC and LHC energies. However, since the masses of the muon and tauon are much larger than that of the electron, the probabilities of producing these heavy leptons are much smaller than for the electron. The clear enhancement at LHC energies is also shown in the these figures.

Finally in Fig. 6, we can see the impact parameter dependence of the probabilities of simultaneous production of all three leptons for RHIC and LHC energies. This plot shows that the probability of simultaneously observing the

three types leptons increases 4 or 5 orders of magnitude at the LHC when compared with the RHIC.

Our results are also in agreement with Ref. [18] for the electron-positron pair production. On the other hand, in Ref. [19] the muon pair production cross sections are slightly greater than our results. The reason for that could be the choice of the nuclear form factors, where they have used the monopole form factor; we have used the Woods-Saxon form factor in the equations.

A recent calculation [21] shows the results of all kinds of lepton pair productions from relativistic heavy ion collisions by using the Monte Carlo program STARLIGHT. In future, it will be possible to compare our results with the results from this program. Heavy leptons, and more than one type of lepton, are produced in the strong fields of ultrarelativistic heavy

ions. As we calculate the cross sections of these productions, it is clear that the cross sections are in the measurable ranges at the LHC. As pointed out in Ref. [22], because of very low transverse momentum  $p_{\perp}$ , it could be difficult to measure these produced leptons. For the next work, it is our task to calculate numerically the transverse momenta of the leptons and compare them with the longitudinal momenta.

#### ACKNOWLEDGMENTS

This research is partially supported by the Istanbul Technical University. We personally thank S. R. Klein for valuable advice in calculating the cross sections and for the careful reading of our article.

- 
- [1] C. Bottcher and M. R. Strayer, *Phys. Rev. D* **39**, 1330 (1989).
  - [2] C. A. Bertulani and G. Baur, *Phys. Rep.* **163**, 299 (1988).
  - [3] M. C. Güçlü, J. C. Wells, A. S. Umar, M. R. Strayer, and D. J. Ernst, *Phys. Rev. A* **51**, 1836 (1995).
  - [4] A. Belkacem and A. H. Sorensen, *Phys. Rev. A* **57**, 3646 (1998).
  - [5] D. Yu. Ivanov, A. Schiller, and V. G. Serbo, *Phys. Lett. B* **454**, 155 (1999).
  - [6] K. Hencken, D. Trautmann, and G. Baur, *Phys. Rev. C* **59**, 841 (1999).
  - [7] C. A. Bertulani, S. R. Klein, and J. Nystrand, *Annu. Rev. Nucl. Part. Sci.* **55**, 271 (2005).
  - [8] A. J. Baltz, S. R. Klein, and J. Nystrand, *Phys. Rev. Lett.* **89**, 012301 (2002).
  - [9] A. J. Baltz, *Phys. Rev. Lett.* **78**, 1231 (1997).
  - [10] M. Y. Sengul, M. C. Guclu, O. Mercan, and N. G. Karakus, *Eur. Phys. J. C* **76**, 428 (2016).
  - [11] J. Adams, M. M. Aggarwal, Z. Ahammed *et al.*, *Phys. Rev. C* **70**, 031902 (2004).
  - [12] C. R. Vane, S. Datz, E. F. Deveney, P. F. Dittner, H. F. Krause, R. Schuch, H. Gao, and R. Hutton, *Phys. Rev. A* **56**, 3682 (1997).
  - [13] S. R. Klein, *Phys. Rev. Spec. Top.* **17**, 121003 (2014).
  - [14] L. Adamczyk, J. K. Adkins, G. Agakishiev *et al.*, *Phys. Lett. B* **750**, 64 (2015).
  - [15] R. C. Barrett and D. F. Jackson, *Nuclear Sizes and Structure* (Oxford University Press, New York, 1977).
  - [16] M. C. Güçlü, *Nucl. Phys. A* **668**, 149 (2000).
  - [17] A. Alscher, K. Hencken, D. Trautmann, and G. Baur, *Phys. Rev. A* **55**, 396 (1997).
  - [18] M. C. Güçlü, J. Li, A. S. Umar, D. J. Ernst, and M. R. Strayer, *Ann. Phys. (N.Y.)* **272**, 7 (1999).
  - [19] G. Baur, K. Hencken, A. Aste, D. Trautmann, and S. R. Klein, *Nucl. Phys. A* **729**, 787 (2003).
  - [20] A. J. Baltz, Y. Gorbunov, S. R. Klein, and J. Nystrand, *Phys. Rev. C* **80**, 044902 (2009).
  - [21] S. R. Klein, J. Nystrand, J. Seger, Y. Gorbunov, and J. Butterworth, *Comput. Phys. Commun.* **212**, 258 (2017).
  - [22] G. Baur, *Eur. Phys. J. D* **55**, 265 (2009).